

---

# **Detecting Anomalous Business Ownership Structures with Graph Neural Networks**

Final Project

Dominic Thorn

## Contents

<b>1</b>	<b>Introduction</b>	<b>5</b>
1.1	Background . . . . .	5
1.2	Aims, Objectives and Research Questions . . . . .	6
1.2.1	Aims . . . . .	6
1.2.2	Objectives . . . . .	6
1.2.3	Research Questions . . . . .	6
1.3	Prior and Related Work . . . . .	6
1.3.1	Detecting Financial Fraud . . . . .	6
1.3.2	Anomaly Detection for Graphs . . . . .	7
1.3.3	Anomalous Node Detection with GNNs . . . . .	8
1.3.4	Recent Developments . . . . .	8
<b>2</b>	<b>Dataset</b>	<b>9</b>
2.1	External Sources . . . . .	9
2.1.1	People with Significant Control Register . . . . .	9
2.1.2	Open Ownership Register . . . . .	9
2.1.3	The Free Company Data Product . . . . .	10
2.2	Initial Data Preparation . . . . .	11
2.3	Graph Generation . . . . .	11
2.3.1	Nodes and Edges . . . . .	11
2.3.2	Connected Components . . . . .	12
2.4	Structural Anomaly Simulation . . . . .	13
2.5	Node Features . . . . .	14
<b>3</b>	<b>Methods</b>	<b>14</b>
3.1	Traditional Machine Learning Approaches to Binary Classification . . . . .	14
3.1.1	Gradient Boosted Trees . . . . .	15
3.2	Graph Neural Networks . . . . .	15
3.2.1	GraphSAGE . . . . .	16
3.2.2	Higher Order GNN (kGNN) . . . . .	17
3.3	Experimental Setup . . . . .	18
3.3.1	Data Splitting . . . . .	18
3.3.2	Class Weighting . . . . .	18
3.3.3	Evaluation Metrics . . . . .	18
3.3.4	Graph Neural Network Training . . . . .	19
3.3.5	CatBoost Training . . . . .	19

<b>4</b>	<b>Results and Discusson</b>	<b>19</b>
4.1	Neural Architecture Search and Hyperparameter Tuning . . . . .	19
4.1.1	GraphSAGE . . . . .	20
4.1.2	kGNN . . . . .	20
4.1.3	CatBoost . . . . .	20
4.2	Model Performance . . . . .	21
<b>5</b>	<b>References</b>	<b>23</b>
<b>6</b>	<b>Appendix</b>	<b>27</b>

## List of Tables

1	Model performance on the test set. . . . .	22
2	Neural architecture search space for GNN models - continuous. . . . .	29
3	Neural architecture search space for GNN models - categorical. . . . .	30

## List of Figures

1	Open Ownership data schema ( <i>Beneficial Ownership Data Standard, 2022</i> ) . . . . .	10
2	Initial distribution of component sizes . . . . .	12
3	Anomaly Simulation Process . . . . .	13
4	Converting homogeneous GNN architectures for heterogeneous learning . . . . .	16
5	GraphSAGE architecture . . . . .	17
6	Hierarchical 1-2-3 GNN network architecture . . . . .	17
7	ROC and PR curves on the test set. . . . .	21
8	Distribution of component sizes. . . . .	27
9	Distribution of anomalous nodes by component size. . . . .	28
10	Distribution of node degrees. . . . .	29

# 1 Introduction

## 1.1 Background

In October of 2021, The International Consortium of Investigative Journalists (ICIJ) revealed the findings of their Pandora Papers investigation. Through examination of nearly 12 million confidential business records, the ICIJ found evidence implicating thousands of individuals and businesses in efforts to conceal the ownership of companies and assets around the world (ICIJ, 2021). The intentions behind this secrecy varied from legitimate privacy concerns to criminal activities, including money laundering, tax evasion, and fraud (European Union Agency for Law Enforcement Cooperation, 2021).

To put these numbers in perspective, a 2019 study by the European Commission estimated that a total of USD 7.8 trillion was held offshore as of 2016. The share of this attributed to the European Union (EU) was USD 1.6 trillion, which corresponds to an estimated tax revenue loss to the EU of EUR 46 billion (European Commission. Directorate General for Taxation and Customs Union., 2019).

Identifying the beneficiaries of a company is challenging due to the ease with which information can be concealed or simply not declared. Further complication is introduced by the interconnected nature of businesses and individuals, as well as the ingenuity of criminals in masking illicit activity. These difficulties place significant strain on the resources of law enforcement agencies and financial institutions (Steven M., 2019).

In April 2016, the United Kingdom made it mandatory for businesses to keep a register of People with Significant Control. This includes people who own more than 25% of the company's shares (*Keeping Your People with Significant Control (PSC) Register*, 2016). Ownership data is curated and processed by the Open Ownership organisation for the purposes of public scrutiny and research (*Open Ownership*, 2022). It is the data provided by Open Ownership that forms the basis of this study. Details of suspicious or illegitimate business owners are not readily available due to the sensitive nature of such records. We propose a method for simulating anomalous ownership structures as part of our experimental methods.

To model the complex network of global business ownership, it is necessary to represent companies, people, and their relationships in a graph structure. With data in this format, it is possible to consider the features of an entity's local neighbourhood when making a decision, in addition to the entity's own characteristics. Anomaly detection algorithms that operate on graph structures remain at the frontier of machine learning research.

To the best of the author's knowledge, there is indeed no published research studying the effectiveness of graph anomaly detection techniques on business ownership networks. The following proposal is a study into the application of state of the art anomaly detection techniques to business ownership graphs.

## **1.2 Aims, Objectives and Research Questions**

### **1.2.1 Aims**

The primary aim of this project is to develop an effective approach for detecting anomalous entities in a business ownership network. Second, the project will offer a comparison of Graph Neural Network (GNN) models to traditional anomaly detection approaches on a business ownership graph. Finally, we contribute a dataset describing a real business ownership network that is suitable for graph learning.

### **1.2.2 Objectives**

- Compose a business ownership graph from open data sources.
- Train and evaluate GNN models for anomaly detection.
- Perform the anomaly detection task with traditional machine learning methods.
- Compare approaches in terms of effectiveness and applicability.

### **1.2.3 Research Questions**

The questions driving the research are as follows:

- What is the most effective strategy for detecting anomalous entities in business ownership networks?
- How do GNN models compare to traditional approaches in terms of classification performance?
- What are the challenges that arise in building and training a GNN model and what recommendations can be made to mitigate these?

## **1.3 Prior and Related Work**

There are few published studies focussed specifically on the detection of anomalous business ownership structures. We offer a review of the most relevant literature below.

### **1.3.1 Detecting Financial Fraud**

Luna et al. (2018) describe a procedure for identifying suspected shell company accounts using distance and density based anomaly detection techniques. The authors were successful in detecting shell companies through observing differences in transactional behaviour. A notable caveat is that the data was simulated for the purposes of the study, which leaves questions around its applicability to real world scenarios.

Recent work by Dumitrescu et al. (2022) demonstrates how local neighbourhood features and statistical scores can be used in Anti-Money Laundering (AML) models. Relevant features included unsupervised anomalous node detection techniques (@ Akoglu et al., 2010) and local neighbourhood connectivity features (Molloy et al., 2016) calculated on *reduced egonets*. A strength of the study is that it was conducted on genuine labelled transactional data with positive results. The authors did not implement any GNN or other deep learning approaches for comparison.

Fronzetti Colladon & Remondi (2017) explore a range of social network analysis techniques for the identification of money laundering using data kept by an Italian factoring company. The authors found that constructing many networks from different projections of the graph entities improved the power of individual risk metrics. Degree centrality was determined to be a significant risk predictor in all cases, while in certain scenarios network constraint proved to be informative. It should be acknowledged that the results obtained are for the clients of a single business and that additional work is required to demonstrate wider validity.

### 1.3.2 Anomaly Detection for Graphs

Akoglu et al. (2014) highlight four main reasons for the suitability of graph structures in anomaly detection:

**Inter-dependent nature of the data** – “Data objects are often related to each other and share dependencies.” This can be observed in business ownership data through the relationships that connect individuals and companies in legal hierarchies and communities.

**Powerful representation** – Graphs offer a powerful way of representing inter-dependencies and long range correlations between related entities. By using different node and edge types, as well as additional attributes, it is possible to represent rich datasets. These properties are valuable in capturing the different types of entities present in a business ownership graph. A business, for example, will have attributes that are not shared by individuals, such as an industry classification code.

**Relational nature of problem domains** – “The nature of anomalies could exhibit themselves as relational”. In context of detecting anomalous business ownership, it is evident that individuals and businesses may be anomalous predominantly through their unusual relationships to other entities.

**Robust machinery** – “Graphs serve as more adversarially robust tools.” It is suggested that graph based systems are ideally suited for fraud detection, as bad actors will find it difficult to alter or fake their position in the global structure.

A thorough description of graph anomaly detection tasks and approaches is offered by X. Ma et al. (2021). Their taxonomy categorises tasks based on the graph component being targeted: nodes, edges, sub-graphs, or full graphs. The authors state their belief that “because the copious types of graph

anomalies cannot be directly represented in Euclidean feature space, it is not feasible to directly apply traditional anomaly detection techniques to graph anomaly detection”.

### 1.3.3 Anomalous Node Detection with GNNs

Kipf & Welling (2017) propose a scalable GNN architecture for classifying nodes in a partially labelled dataset. Early attempts to apply deep learning to graph structures utilised RNN architectures which prove difficult to scale (Gori et al., 2005; Li et al., 2017; Scarselli et al., 2009). Kipf et al. extend prior work on spectral GNNs (Bruna et al., 2014; Defferrard et al., 2017) to produce a flexible model that scales in linear time with respect to the number of graph edges.

Ding et al. (2019) combine a GNN architecture with an autoencoder in a method that identifies anomalous nodes by reconstruction error. The proposed method, DOMINANT, uses a GNN to generate node embeddings and separately reconstructs both the graph topology and the node attributes. This strategy is further developed and applied to multi-view data through the combination of multiple graph encoders (Peng et al., 2022).

An alternative method is offered by Li et al. (2019), in which a spectral convolution and deconvolution framework is used to identify anomalous nodes in conjunction with a density estimation model. The approach continues to demonstrate the importance of combining multiple perspectives of the network data, with the innovation being the use of a Gaussian Mixture Model to combine representations in a single view.

### 1.3.4 Recent Developments

Veličković et al. (2018) demonstrate the use of self-attention layers to address shortcomings in the representations captured by GNN architectures. However, a comparison of Relational Graph Attention (GAT) models to GNNs showed that relative performance was task dependent and that current GAT models could not be shown to consistently outperform GNNs on benchmark exercises (Busbridge et al., 2019).

In an application of graph attention based models to financial fraud detection, Wang et al. (2019) show that their SemiGNN model outperforms established approaches when predicting risk of default and in attribute prediction. Baseline methods used for comparison included a XGBoost (Chen & Guestrin, 2016), GNN, GAT, and LINE (Tang et al., 2015).

The GraphSAGE (**hamiltonInductiveRepresentationLearning2017?**) node embedding framework is among the most popular



## 2 Dataset

Training a supervised classification model requires access to a dataset of labelled examples. Given the typical infrequency of fraudulent events to legitimate cases, it is common for fraud classification projects require large amounts of data in order to provide a modest number of fraudulent examples from which the model can learn. However, considering the sensitive nature of fraud investigations, it is not surprising to find that no such data is available in the public domain.

In the following section we detail the public data sources used in this study and the steps necessary for processing them. We further propose a method for simulating anomalous business ownership structures using this publically available data.

### 2.1 External Sources

#### 2.1.1 People with Significant Control Register

Since 2016, it has been a requirement for all businesses in the United Kingdom to declare People of Significant Control (PSC) (*Keeping Your People with Significant Control (PSC) Register*, 2016). This includes all shareholders with ownership greater than 25%, any persons with more than 25% of voting rights, and any person with the right to appoint or remove the majority of the board of directors (*People with Significant Control (PSCs)*, 2022). The register is available as a daily snapshot, available to download from the Companies House webpage (*Companies House*, 2022).

Included in the register are the name, address, and identification number of each company for which a declaration has been received. Also listed are the name, address, country of origin, date of birth, and nature of control for each person listed as a PSC.

Rather than consume this data directly, we obtain this information from a data feed curated by the Open Ownership organisation.

#### 2.1.2 Open Ownership Register

The Open Ownership organisation maintains a database of over 16 million beneficial ownership records, including those collated in the UK PSC register and from additional sources made available by other countries (*Open Ownership*, 2022). This data is provided in a standardised format that is conducive to machine processing and graph generation. Additional data quality processing is undertaken by Open Ownership, such as the merging of duplicated records for persons that have more than one PSC declaration (*Beneficial Ownership Data Standard*, 2022).

The Open Ownership Register is used as a canonical source of company, person, and ownership relationships for the generation of our UK business ownership graph.

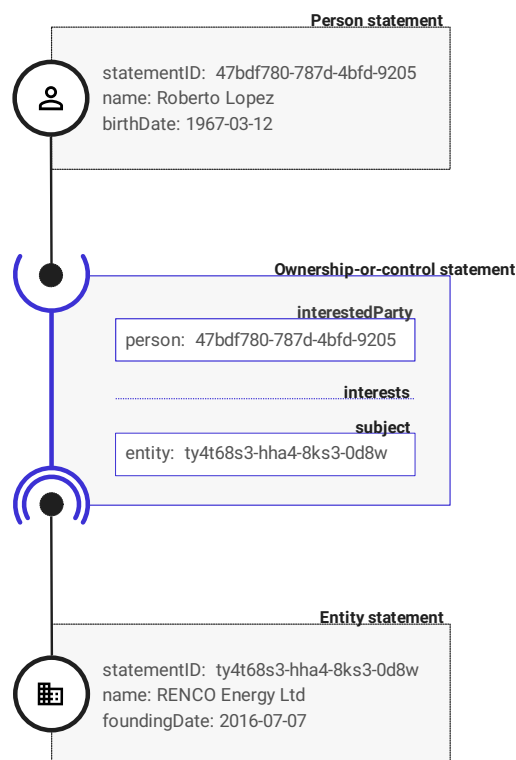


**Figure 1:** Open Ownership data schema (*Beneficial Ownership Data Standard, 2022*)

### 2.1.3 The Free Company Data Product

The Free Company Data Product is a monthly snapshot of data for all live companies on the UK public register. Taken from the Companies House data products website, this data includes:

- basic information including company type and registered office address
- the nature of business or standard industrial classification (SIC)
- company status, such as ‘live’ or ‘dissolved’
- date of last accounts or confirmation statement filed
- date of next accounts or confirmation statement due
- previous company names

(*Companies House Data Products, n.d.*)

This data serves as an additional source of node features for company entities in the generated dataset.

## 2.2 Initial Data Preparation

The Open Ownership data file consists of over 20 million records stored as nested JSON objects. This includes data for businesses and relevant persons registered outside of the UK. The Apache Spark framework (*Apache Spark*, 2022) is used for bulk data preparation due to its parallel and out-of-core processing capabilities, as well as its support for nested data structures.

As the scope of this study covers only UK registered companies and their shareholders, records for entities that do not have a shareholding interest in a UK company are discarded. Non-UK companies that are registered as a shareholder of a UK company are also discarded, as we are unable to obtain information for these entities via Companies House. Computational resource constraints also prevent handling of a larger dataset. To further limit dataset size, and in the interests of only considering accurate and up to date information, we also filter out companies that are listed as dissolved.

While the initial nested data schema is desirable for clean representation and compact storage, we require a flat relational table structure for analytical and model training purposes. Relevant data items are extracted into a flat table for each entity type. This results in three tables of interim output: company information, person information, and statements of control that link entities to their ownership interests.

The Companies House data is joined to the company entity table via the UK company registration number.

## 2.3 Graph Generation

### 2.3.1 Nodes and Edges

The company, person, and ownership relationship tables prepared in the previous steps are used to create a graph data structure. Companies and persons are represented as nodes in the graph, and the ownership relationships represented as directed edges (from owner to owned entity) between them. The resulting graph is attributed with node features and edge weights. Since the graph consists of two types of nodes with distinct feature sets, it can be described as an attributed heterogeneous graph (X. Ma et al., 2021).

### 2.3.2 Connected Components

Connected components are labelled in the graph to facilitate additional filtering and to allow for parallel computation of topological features.

Two nodes,  $u$  and  $v$ , are considered to be connected if a path exists between them in the graph  $G$ . If no path exists between  $u$  and  $v$  then they are said to be disconnected. Not all entities in the ownership graph are connected by any path, and so the ownership graph  $G$  can be viewed as a set of disjoint sets of nodes, or components. The graph  $G = (V, E)$  is described by its components thus:  $G[V_1], G[V_2], \dots G[V_\omega]$ . If the number of nodes in a graph is denoted by  $|V|$ , the number of nodes in a component  $\omega$  can be described by  $|V_\omega|$  (Bondy & Murty, 1982, p. 13).

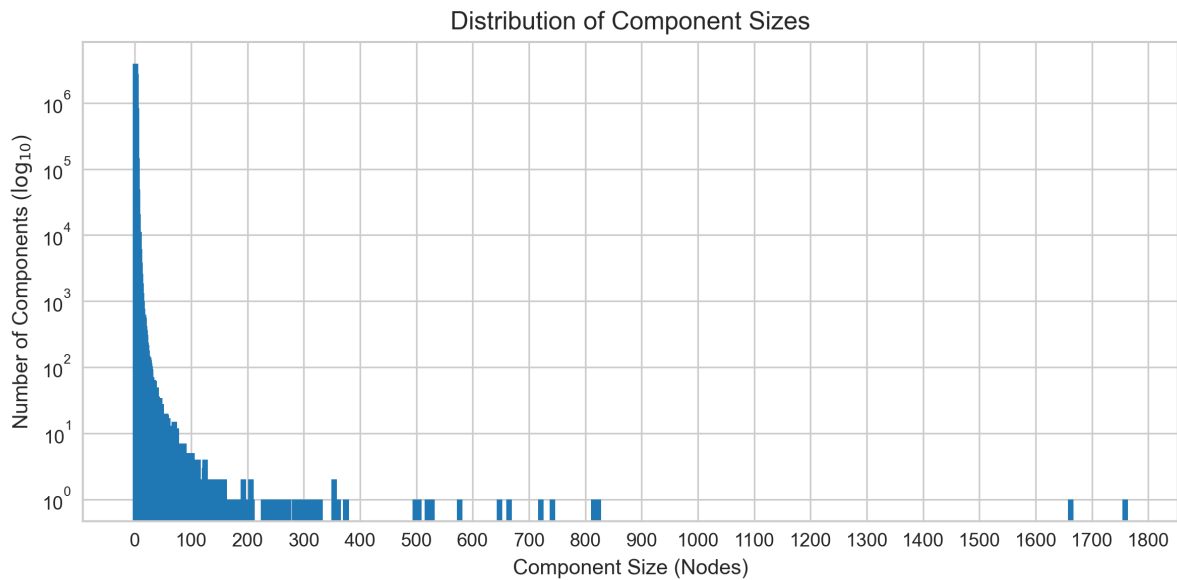


**Figure 2:** Initial distribution of component sizes. A single super-component consisting of 27,008 nodes is excluded from the plot.

The vast majority of businesses in the dataset have only one or two declared PSC shareholders. The initial distribution of component sizes is shown in figure 2. These small subgraphs are not of interest in this study and are excluded, along with any component that contains fewer than ten nodes or with a ratio of less than 1 in 10 natural persons to companies.

The rationale for excluding these components is threefold: first, the small number of nodes and relationships presents little information for a model to learn from; second, these small networks are less likely to be of interest in real world fraud detection, as illegitimate ownership is usually concealed behind multiple layers of ownership; and from a practical standpoint, the volume of data is brought down to a manageable size. Networks with fewer than 1 in 10 natural persons to companies are excluded,

as a focus of this study is on the performance of anomaly detection methods on heterogeneous graph data, as opposed to homogeneous networks.

Finally, we address an observed data quality issue in which multiple nodes in the same component may share the same name. These nodes are merged into a single node, with the resulting node taking on all the ownership relationships of the merged nodes.

## 2.4 Structural Anomaly Simulation

To simulate structural anomalies, 10% of the nodes are selected at random and marked as anomalous ( $y = 1$ ) and the remaining 90% marked as normal ( $y = 0$ ). A single outgoing edge is chosen from each anomalous node,  $\epsilon_{norm} = \epsilon(u_i, v_i)$ , and its source ID replaced with that of another node marked as anomalous,  $u_j$ . This produces the new anomalous edge  $\epsilon_{anom} = \epsilon(u_j, v_i)$  and eliminates the original edge  $\epsilon_{norm}$ . The result is an exchanging of ownership interests between anomalous nodes, while preserving the overall structure of the graph. The procedure is illustrated in figure 3. This process is repeated until all anomalous nodes have one edge replaced with a different edge so that for all anomalous nodes  $\epsilon_{anom} \neq \epsilon_{norm}$ . The outgoing edges of normal nodes are not altered, though their incoming edges may be affected by the anomaly simulation process.

The final step of the simulation is to discard any small components ( $n < 9$ ) that have been created as a result of the anomaly simulation process. This is done to ensure that anomalous nodes belong to components with a similar size distribution to the original graph, as demonstrated in figures 8 and 9. The final proportion of anomalous nodes in the simulated graph is 7.3%.

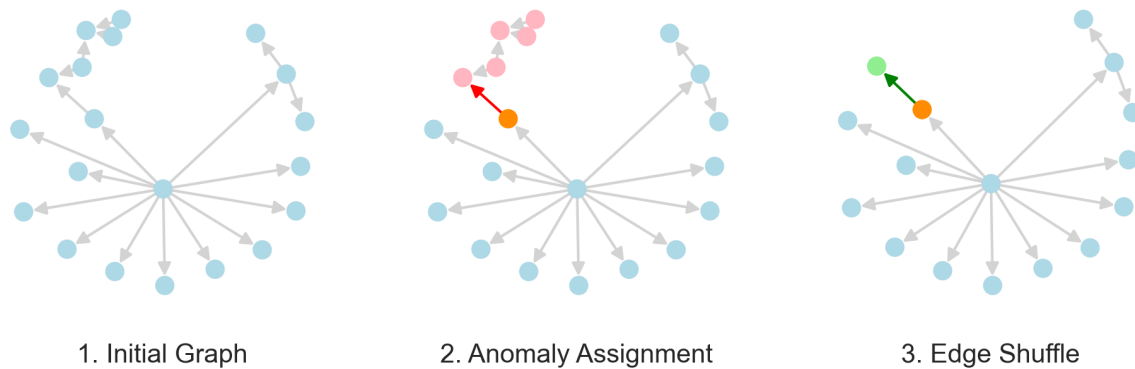


**Figure 3:** Process for simulating structural anomalies. The initial graph is shown in (1). A node is selected for anomalisation (orange circle) in (2). The outgoing edge (red arrow) is swapped for that of another anomalised node (green arrow), resulting in the exchange of pink nodes for green (3).

The anomaly simulation process introduces unusual ownership relationships into the graph. The true

frequency of these occurrences is unknown, but is expected to be far lower than 7.3% of nodes. This anomaly rate is chosen to ensure that model training is not impossible due to extreme class imbalance, and the same effect can be achieved by oversampling the minority class (Chawla et al., 2002) or undersampling the majority class (Fernández, 2018, p. 82).

When labelling the unaltered nodes as normal, it is assumed that the data originally provided by Open Ownership is accurate and that if any anomalies are present they will have a negligible impact on experimental results. Nevertheless, anomalies in the initial dataset will be seen by all candidate models, and so should not bias the results.

### 2.5 Node Features

In order to train a baseline model for comparison, a set of node level features is generated to represent each node in a tabular format (Leskovec, 2021). The following topological features are extracted for each node:

- Indegree: The number of incoming edges to the node.
- Outdegree: The number of outgoing edges from the node.
- Closeness Centrality: Inverse of the sum of shortest path distances to all other nodes.
- Clustering Coefficient: Connectedness of neighbouring nodes.
- PageRank: A measure of node importance, based on the importance of neighbouring nodes (Page et al., 1998).

To capture information about the node's position in the graph, aggregate statistics are calculated for the aforementioned topological features for the node's neighbours and added as features:

- Minimum
- Maximum
- Sum
- Mean
- Standard Deviation

The count of immediate neighbours is also included as a feature.

## 3 Methods

### 3.1 Traditional Machine Learning Approaches to Binary Classification

In order to assess the relative improvement that can be achieved by using Graph Neural Networks, we compare their performance to a baseline model trained on a set of node level features.

### 3.1.1 Gradient Boosted Trees

Gradient boosted tree ensembles achieve robust performance on a wide range of machine learning tasks (Friedman, 2001). Modern applications are favoured for their strong performance in capturing complex dependencies, native handling of heterogeneous and missing data, and numerical scale invariance. We use the CatBoost library to train our baseline model, as the current state-of-the-art implementation (Prokhorenkova et al., 2019).

## 3.2 Graph Neural Networks

The PyTorch Geometric library offers a comprehensive set of methods for deep learning on graph data structures (Fey & Lenssen, 2019). We use the implementations provided in this library to train our Graph Neural Network models.

We select two architectures, GraphSAGE (Hamilton et al., 2018) and kGNN (Morris et al., 2021), for our experiment. These models are chosen for their demonstrated performance at node classification tasks and ability to handle heterogeneous graph data with slight modification (detailed below) Morris et al. (2021). A further consideration in this choice of models is the size of our dataset and the available computational resources. Both architectures are relatively lightweight compared to other models, such as Graph Attention Networks (velivckovicGraphAttentionNetworks2018?), and can be trained on a single GPU in a reasonable amount of time.

Since both GNN architectures selected for this study were originally implemented for learning on homogeneous graphs, we use a method provided by PyTorch Geometric for adapting these homogeneous architectures for learning on our heterogeneous dataset. A homogeneous model is adapted for heterogeneous learning by duplicating message passing functions to operate on each edge type individually. Node representations are learned for each node type and aggregated using a user provided function that we choose via neural architecture search. This technique is described by Schlichtkrull et al. (2017)

and illustrated in figure 4.

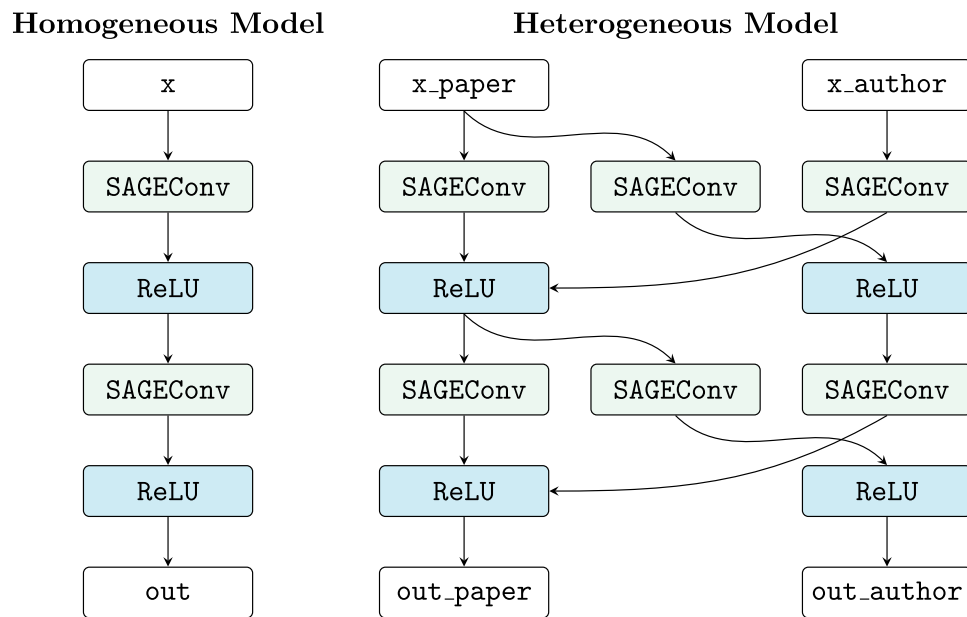


**Figure 4:** Converting homogeneous GNN architectures for heterogeneous learning (*Heterogeneous Graph Learning – PyTorch Geometric Documentation*, n.d.)

### 3.2.1 GraphSAGE

The GraphSAGE model proposed by Hamilton et al. (2018) is a node embedding framework that uses both node attributes and the attributes of neighbouring nodes to generate node representations. During training, the model learns how to effectively aggregate information from the neighbourhood of each node and combine this with the node’s own features to produce a learned representation.

The aggregation architecture can be any symmetric function, such as the mean or sum, or a more complex function such as a neural network that can operate on an ordered set of node features. For supervised learning tasks, the parameters of the aggregation function are learned via backpropagation.



Edge attributes are not used in the GraphSAGE model and are therefore ignored during training.

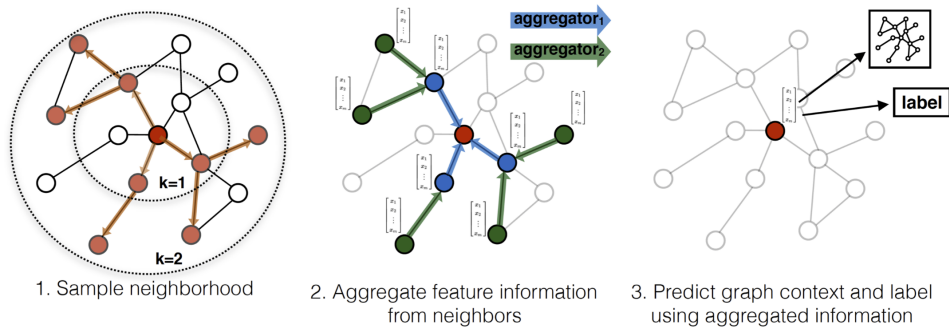


**Figure 5:** GraphSAGE neighbourhood sampling and aggregation (Hamilton et al., 2018)

### 3.2.2 Higher Order GNN (kGNN)

The Higher-Order GNN (or kGNN) proposed by Morris et al. (2021) is an extension of the prototypical GNN described by Kipf & Welling (2017) to higher order graph representations. These higher order representations are learned by associating all unordered  $k$ -tuples of nodes and learning a representation for each tuple, where  $k$  is a hyperparameter of the model. These tuple representations are hierarchically combined in a final dense layer to produce a representation for each node that takes into account its local neighbourhood and higher order topological features. This is illustrated in figure 6.

As with the GraphSAGE model, an aggregation architecture is used to learn the node tuple representations. The weights for each layer are also trained via backpropagation for supervised learning tasks. Unlike the GraphSAGE model, the kGNN model does incorporate edge weights in its learning process.

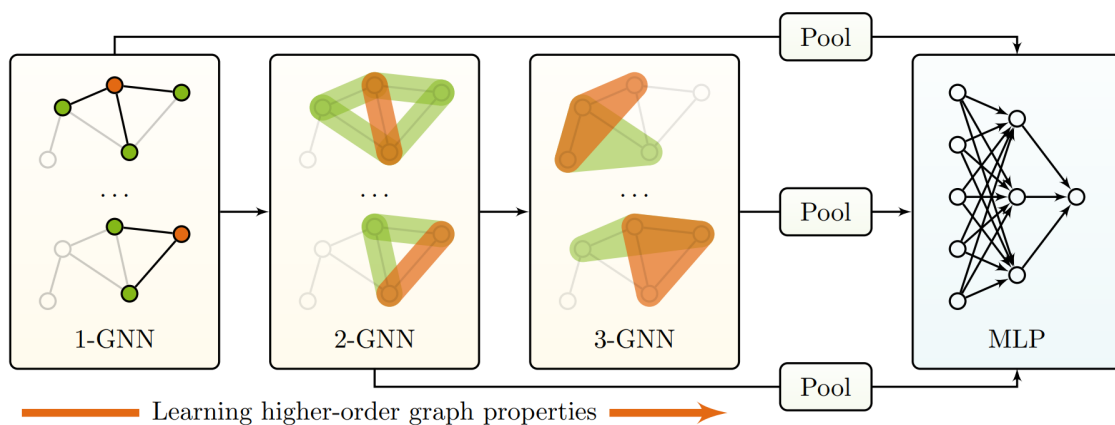


**Figure 6:** Hierarchical 1-2-3 GNN network architecture (Morris et al., 2021)

### 3.3 Experimental Setup

#### 3.3.1 Data Splitting

The dataset is split into training, validation, and test sets. The training set is used to train the model, the validation set is used to tune hyperparameters, and the test set is used to evaluate the model's performance. The split is performed using a random 80/10/10 split, with random selection applied to each component in the graph to ensure that nodes in the same component are not split across multiple sets.

#### 3.3.2 Class Weighting

Class imbalance in the dataset is addressed by assigning a weight to each class during model training. A weight of 10 is applied to anomalous nodes and a weight of 1 for normal nodes. These weights are used as multipliers for the errors of their respective classes, leading to increased penalty and greater emphasis for anomalous nodes. This is a cost sensitive approach to class imbalance that conveniently does not require the use of oversampling or undersampling (He & Garcia, 2009).

#### 3.3.3 Evaluation Metrics

We use two threshold-free metrics to evaluate model performance: the area under the precision-recall curve (AUC-PR) and the area under the receiver operating characteristic curve (AUC-ROC). These metrics are chosen as they are insensitive to the choice of threshold, and are more robust to class imbalance than threshold dependent metrics such as accuracy. (Y. Ma & He, 2013, p. 72)

**3.3.3.1 Area under the Receiver Operating Characteristic Curve (AUC-ROC)** The Receiver Operating Characteristic Curve (ROC) is a plot of the true positive rate against the false positive rate along a range of threshold settings. A perfect model will achieve a 100% true positive rate with a 0% false positive rate, while a zero-skill classifier will achieve a 50% true positive rate with a 50% false positive rate. The area under the ROC curve (AUC-ROC) provides a way to summarise model performance over the range of threshold values. A perfect model will have an AUC-ROC of 1, while the zero-skill model will have an AUC-ROC of 0.5. (Fawcett, 2006)

**3.3.3.2 Area under the Precision-Recall Curve (AUC-PR)** The Precision-Recall Curve (PR) is a plot of precision against recall along the range of recall values. A perfect model will achieve a 100% precision and 100% recall, while a zero-skill classifier will achieve a rate of precision equal to the proportion of positive cases in the dataset along for all recall values. The area under the PR curve (AUC-PR) provides

a way to summarise model performance over the range of recall values. A perfect model will have an AUC-PR of 1, while the zero-skill model will have an AUC-PR equal to the proportion of positive cases in the dataset. The PR curve can provide a more accurate view of model performance on imbalanced datasets. (Saito & Rehmsmeier, 2015)

### 3.3.4 Graph Neural Network Training

**3.3.4.1 Optimiser** The Adam optimiser (Kingma & Ba, 2017) is used to train the GNNs with an initial learning rate of 0.01.

**3.3.4.2 Neural Architecture Search** For each of the GNN models (GraphSAGE and kGNN), we learn an optimal neural architecture for the anomalous node classification task. We use the Optuna library (Akiba et al., 2019) to explore the search space, training candidate models on the training dataset and selecting the architecture that achieves the highest AUC-PR on the validation data.

Each model is trained for a maximum of 2000 epochs, with an early stopping callback used to terminate trials that do not improve for 200 consecutive epochs. Thirty trials are performed for each model. Both GNN models share the same search spaces, the parameters of the space are provided in the appendix tables 2 and 3.

**3.3.4.3 Hyperparameter Tuning** Parameters for dropout and weight decay are also tuned using Optuna. These trials take place after the architecture search, in order to limit the dimensionality of the search space in each experiment. A total of 20 trials are performed for each pair of candidate values, with the best hyperparameters selected based on the AUC-PR score on the validation set.

### 3.3.5 CatBoost Training

The CatBoost classifier is trained in a similar manner to the GNNs. Each candidate model is trained and evaluated on the same training and validation sets as the GNN models, and evaluated using the AUC-PR metric. The hyperparameter search space is provided in the appendix table ??.

## 4 Results and Discussion

### 4.1 Neural Architecture Search and Hyperparameter Tuning

It was observed during the model tuning process that both GNN models displayed a great deal of variance in performance, even between trials when all hyperparameters were held constant. This suggests

a high deal of sensitivity to the initialisation of the model weights, and that the model architecture is not the only factor in determining model performance.

In order to ensure that the final model is among the best possible candidates, we perform several round of training with the best performing architecture, checking validation performance at each epoch and saving the weights whenever the validation AUC-PR improves beyond the previous best. This process is repeated for each of the GNN models, and the final model is selected based on the best validation AUC-PR score. This is in contrast to the commonly adopted strategy of training the final model for a predetermined number of epochs on both the training and validation datasets.

Further, it was noted that both models exhibited a non-linear progression in performance over the course of training and showed no signs of overfitting. While this could suggest that the models have not converged, allowing the models to train over thousands of epochs showed that the validation AUC-PR continues to increase and decrease in a non-linear fashion. It may be worth studying this behaviour in future work to determine whether it is a result of the model architecture, the dataset, or some other factor in the experimental design.

### **4.1.1 GraphSAGE**

The best performing architecture for the GraphSAGE models was found to be a 2-layer model with 256 hidden channels, a bias term, and an additional linear layer after the final message passing layer. A sum aggregation function was selected for both the message passing layers and for the aggregation of heterogeneous node representations. A leaky relu activation function was selected for all layers. Neither dropout nor weight decay were found to be beneficial to model performance.

### **4.1.2 kGNN**

The best performing architecture for the kGNN model was found to be a 4-layer model with 128 hidden channels, no bias term, and an additional linear layer after the final message passing layer. A minimum pooling aggregation function was selected for both the message passing layers and for the aggregation of heterogeneous node representations. A gelu activation function was selected for all layers. Neither dropout nor weight decay were found to be beneficial to model performance.

### **4.1.3 CatBoost**

The most successful CatBoost model was found to have the following parameters:

- learning rate: 0.09
- depth: 9

- boosting\_type: Plain
- bootstrap\_type: MVS
- colsample\_bylevel: 0.08

## 4.2 Model Performance

Both of the GNN models achieved significantly higher AUC-ROC and AUC-PR scores than the CatBoost model. The kGNN model achieved the highest AUC-ROC and AUC-PR scores, with an AUC-ROC of 0.982 and an AUC-PR of 0.904. The GraphSAGE model achieved an AUC-ROC of 0.953 and an AUC-PR of 0.767. The CatBoost model achieved an AUC-ROC of 0.639 and an AUC-PR of 0.104.

95% confidence intervals are provided for the AUC-ROC and AUC-PR scores. These are calculated using the bootstrap method (*Davison, n.d.*) for 10,000 iterations.

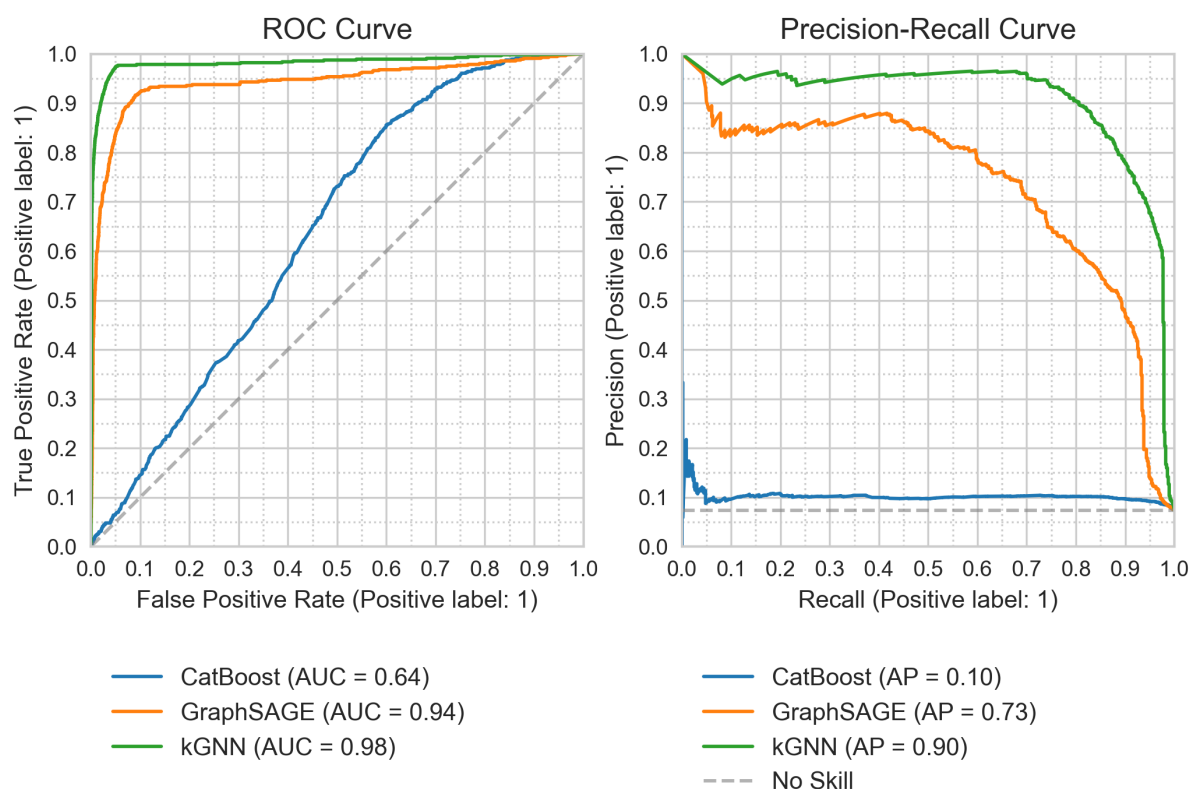


**Figure 7:** ROC and PR curves on the test set.

**Table 1:** Model performance on the test set.

Model	AUC-ROC	95% CI	AUC-PR	95% CI
CatBoost	0.639	[0.619, 0.659]	0.104	[0.092, 0.116]
GraphSAGE	0.943	[0.929, 0.957]	0.735	[0.695, 0.775]
kGNN	<b>0.982</b>	[0.974, 0.990]	<b>0.904</b>	[0.876, 0.932]

The stand out performance of the kGNN model may be explained by its capacity to learn and combine higher order features of the graph. A potential avenue for further study would be to investigate what features the model is learning and how they influence the model's performance. Work by Ying et al. (2019) on the GNNExplainer tool is likely worth exploring.

It should also be noted that the kGNN model has two additional message passing layers compared to the GraphSAGE model. This may be a contributing factor to the model's superior performance, however the kGNN consists of half as many hidden channels. This model depth may be another contributing factor to the model's superior performance.

## 5 References

- Akiba, T., Sano, S., Yanase, T., Ohta, T., & Koyama, M. (2019). *Optuna: A Next-generation Hyperparameter Optimization Framework* (No. arXiv:1907.10902). arXiv. <https://doi.org/10.48550/arXiv.1907.10902>
- Akoglu, L., McGlohon, M., & Faloutsos, C. (2010). Oddball: Spotting Anomalies in Weighted Graphs. In M. J. Zaki, J. X. Yu, B. Ravindran, & V. Pudi (Eds.), *Advances in Knowledge Discovery and Data Mining* (Vol. 6119, pp. 410–421). Springer Berlin Heidelberg. [https://doi.org/10.1007/978-3-642-13672-6\\_40](https://doi.org/10.1007/978-3-642-13672-6_40)
- Akoglu, L., Tong, H., & Koutra, D. (2014). *Graph-based Anomaly Detection and Description: A Survey* (No. arXiv:1404.4679). arXiv. <https://doi.org/10.48550/arXiv.1404.4679>
- Apache Spark: A unified engine for big data processing: Communications of the ACM: Vol 59, No 11.* (2022, June 13). <https://dl.acm.org/doi/10.1145/2934664>
- Beneficial Ownership Data Standard.* (2022, September 18). openownership.org. <https://www.openownership.org/en/topics/beneficial-ownership-data-standard/>
- Bondy, A., & Murty, U. S. R. (1982). *Graph Theory*. Springer London. <https://books.google.com?id=5Z71jwEACAAJ>
- Bruna, J., Zaremba, W., Szlam, A., & LeCun, Y. (2014). *Spectral Networks and Locally Connected Networks on Graphs* (No. arXiv:1312.6203). arXiv. <https://doi.org/10.48550/arXiv.1312.6203>
- Busbridge, D., Sherburn, D., Cavallo, P., & Hammerla, N. Y. (2019). *Relational Graph Attention Networks* (No. arXiv:1904.05811). arXiv. <https://doi.org/10.48550/arXiv.1904.05811>
- Chawla, N. V., Bowyer, K. W., Hall, L. O., & Kegelmeyer, W. P. (2002). SMOTE: Synthetic Minority Over-sampling Technique. *Journal of Artificial Intelligence Research*, 16, 321–357. <https://doi.org/10.1613/jair.953>
- Chen, T., & Guestrin, C. (2016). XGBoost: A Scalable Tree Boosting System. *Proceedings of the 22nd ACM SIGKDD International Conference on Knowledge Discovery and Data Mining*, 785–794. <https://doi.org/10.1145/2939672.2939785>
- Companies House.* (2022, June 12). [http://download.companieshouse.gov.uk/en\\_pscdata.html](http://download.companieshouse.gov.uk/en_pscdata.html)
- Companies House data products.* (n.d.). GOV.UK. Retrieved September 18, 2022, from <https://www.gov.uk/guidance/companies-house-data-products>
- Davison: Bootstrap methods and their application - Google Scholar.* (n.d.). Retrieved September 19, 2022, from [https://scholar.google.com/scholar\\_lookup?&title=Bootstrap%20methods%20and%20the%20application&publication\\_year=1997&author=Davison%2CAC&author=Hinkley%2CDV](https://scholar.google.com/scholar_lookup?&title=Bootstrap%20methods%20and%20the%20application&publication_year=1997&author=Davison%2CAC&author=Hinkley%2CDV)
- Defferrard, M., Bresson, X., & Vandergheynst, P. (2017). *Convolutional Neural Networks on Graphs with Fast Localized Spectral Filtering* (No. arXiv:1606.09375). arXiv. <https://doi.org/10.48550/arXiv.1606.09375>

- Ding, K., Li, J., Bhanushali, R., & Liu, H. (2019). *Deep Anomaly Detection on Attributed Networks* (pp. 594–602). <https://doi.org/10.1137/1.9781611975673.67>
- Dumitrescu, B., Băltoiu, A., & Budulan, Ș. (2022). Anomaly Detection in Graphs of Bank Transactions for Anti Money Laundering Applications. *IEEE Access*, 10, 47699–47714. <https://doi.org/10.1109/ACCESS.2022.3170467>
- European Commission. Directorate General for Taxation and Customs Union. (2019). *Estimating international tax evasion by individuals*. Publications Office. <https://data.europa.eu/doi/10.2778/300732>
- European Union Agency for Law Enforcement Cooperation. (2021). *Shadow money: The international networks of illicit finance*. [https://op.europa.eu/publication/manifestation\\_identifier/PUB\\_QLAN21003ENN](https://op.europa.eu/publication/manifestation_identifier/PUB_QLAN21003ENN)
- Fawcett, T. (2006). An introduction to ROC analysis. *Pattern Recognition Letters*, 27(8), 861–874. <https://doi.org/10.1016/j.patrec.2005.10.010>
- Fernández. (2018). *Learning from Imbalanced Data Sets* (1st ed. 2018 edition). Springer.
- Fey, M., & Lenssen, J. E. (2019). *Fast Graph Representation Learning with PyTorch Geometric* (No. arXiv:1903.02428). arXiv. <https://doi.org/10.48550/arXiv.1903.02428>
- Friedman, J. H. (2001). Greedy function approximation: A gradient boosting machine. *Annals of Statistics*, 1189–1232.
- Fronzetti Colladon, A., & Remondi, E. (2017). Using social network analysis to prevent money laundering. *Expert Systems with Applications*, 67, 49–58. <https://doi.org/10.1016/j.eswa.2016.09.029>
- Gori, M., Monfardini, G., & Scarselli, F. (2005). A new model for learning in graph domains. In *Proceedings of the International Joint Conference on Neural Networks* (Vol. 2, pp. 734 vol. 2). <https://doi.org/10.1109/IJCNN.2005.1555942>
- Hamilton, W. L., Ying, R., & Leskovec, J. (2018). *Inductive Representation Learning on Large Graphs* (No. arXiv:1706.02216). arXiv. <https://doi.org/10.48550/arXiv.1706.02216>
- He, H., & Garcia, E. A. (2009). Learning from Imbalanced Data. *IEEE Transactions on Knowledge and Data Engineering*, 21(9), 1263–1284. <https://doi.org/10.1109/TKDE.2008.239>
- Heterogeneous Graph Learning — PyTorch Geometric documentation*. (n.d.). Retrieved September 19, 2022, from <https://pytorch-geometric.readthedocs.io/en/latest/notes/heterogeneous.html>
- ICIJ. (2021, October 3). *Offshore havens and hidden riches of world leaders and billionaires exposed in unprecedented leak - ICIJ*. <https://www.icij.org/investigations/pandora-papers/global-investigation-tax-havens-offshore/>



- Keeping your people with significant control (PSC) register*. (2016, April 6). GOV.UK. <https://www.gov.uk/government/news/keeping-your-people-with-significant-control-psc-register>
- Kingma, D. P., & Ba, J. (2017). *Adam: A Method for Stochastic Optimization* (No. arXiv:1412.6980). arXiv. <https://doi.org/10.48550/arXiv.1412.6980>
- Kipf, T. N., & Welling, M. (2017). *Semi-Supervised Classification with Graph Convolutional Networks* (No. arXiv:1609.02907). arXiv. <https://doi.org/10.48550/arXiv.1609.02907>
- Leskovec, J. (2021). *Traditional Methods for Machine Learning in Graphs*. Lecture. <http://snap.stanford.edu/class/cs224w-2020/slides/02-tradition-ml.pdf>
- Li, Y., Huang, X., Li, J., Du, M., & Zou, N. (2019). *SpecAE: Spectral AutoEncoder for Anomaly Detection in Attributed Networks* (No. arXiv:1908.03849). arXiv. <https://doi.org/10.48550/arXiv.1908.03849>
- Li, Y., Tarlow, D., Brockschmidt, M., & Zemel, R. (2017). *Gated Graph Sequence Neural Networks* (No. arXiv:1511.05493). arXiv. <https://doi.org/10.48550/arXiv.1511.05493>
- Luna, D. K., Palshikar, G. K., Apte, M., & Bhattacharya, A. (2018). Finding shell company accounts using anomaly detection. *Proceedings of the ACM India Joint International Conference on Data Science and Management of Data*, 167–174. <https://doi.org/10.1145/3152494.3152519>
- Ma, X., Wu, J., Xue, S., Yang, J., Zhou, C., Sheng, Q. Z., Xiong, H., & Akoglu, L. (2021). *A Comprehensive Survey on Graph Anomaly Detection with Deep Learning*. <http://arxiv.org/abs/2106.07178>
- Ma, Y., & He, H. (Eds.). (2013). *Imbalanced Learning: Foundations, Algorithms, and Applications* (1st edition). Wiley-IEEE Press.
- Molloy, I., Chari, S., Finkler, U., Wiggerman, M., Jonker, C., Habeck, T., Park, Y., Jordens, F., & Schaik, R. (2016, February 22). *Graph Analytics for Real-time Scoring of Cross-channel Transactional Fraud*.
- Morris, C., Ritzert, M., Fey, M., Hamilton, W. L., Lenssen, J. E., Rattan, G., & Grohe, M. (2021). *Weisfeiler and Leman Go Neural: Higher-order Graph Neural Networks* (No. arXiv:1810.02244). arXiv. <https://doi.org/10.48550/arXiv.1810.02244>
- Open Ownership*. (2022, May 24). openownership.org. <https://www.openownership.org/en/>
- Page, L., Brin, S., Motwani, R., & Winograd, T. (1998). *The PageRank Citation Ranking: Bringing Order to the Web*.
- Peng, Z., Luo, M., Li, J., Xue, L., & Zheng, Q. (2022). A Deep Multi-View Framework for Anomaly Detection on Attributed Networks. *IEEE Transactions on Knowledge and Data Engineering*, 34(6, 6), 2539–2552. <https://doi.org/10.1109/TKDE.2020.3015098>
- People with significant control (PSCs)*. (2022, September 18). GOV.UK. <https://www.gov.uk/guidance/people-with-significant-control-pscs>

- Prokhorenkova, L., Gusev, G., Vorobev, A., Dorogush, A. V., & Gulin, A. (2019). *CatBoost: Unbiased boosting with categorical features* (No. arXiv:1706.09516). arXiv. <https://doi.org/10.48550/arXiv.1706.09516>
- Saito, T., & Rehmsmeier, M. (2015). The Precision-Recall Plot Is More Informative than the ROC Plot When Evaluating Binary Classifiers on Imbalanced Datasets. *PLOS ONE*, 10(3), e0118432. <https://doi.org/10.1371/journal.pone.0118432>
- Scarselli, F., Gori, M., Tsoi, A. C., Hagenbuchner, M., & Monfardini, G. (2009). The Graph Neural Network Model. *IEEE Transactions on Neural Networks*, 20(1, 1), 61–80. <https://doi.org/10.1109/TNN.2008.2005605>
- Schlichtkrull, M., Kipf, T. N., Bloem, P., Berg, R. van den, Titov, I., & Welling, M. (2017). *Modeling Relational Data with Graph Convolutional Networks* (No. arXiv:1703.06103). arXiv. <https://doi.org/10.48550/arXiv.1703.06103>
- Steven M., D. (2019, May 21). *Combating Illicit Financing by Anonymous Shell Companies — FBI* [Testimony]. <https://www.fbi.gov/news/testimony/combating-illicit-financing-by-anonymous-shell-companies>
- Tang, J., Qu, M., Wang, M., Zhang, M., Yan, J., & Mei, Q. (2015). LINE: Large-scale Information Network Embedding. *Proceedings of the 24th International Conference on World Wide Web*, 1067–1077. <https://doi.org/10.1145/2736277.2741093>
- Veličković, P., Cucurull, G., Casanova, A., Romero, A., Liò, P., & Bengio, Y. (2018). *Graph Attention Networks* (No. arXiv:1710.10903). arXiv. <http://arxiv.org/abs/1710.10903>
- Wang, D., Lin, J., Cui, P., Jia, Q., Wang, Z., Fang, Y., Yu, Q., Zhou, J., Yang, S., & Qi, Y. (2019). A Semi-supervised Graph Attentive Network for Financial Fraud Detection. *2019 IEEE International Conference on Data Mining (ICDM)*, 598–607. <https://doi.org/10.1109/ICDM.2019.00070>
- Ying, R., Bourgeois, D., You, J., Zitnik, M., & Leskovec, J. (2019). *GNNExplainer: Generating Explanations for Graph Neural Networks* (No. arXiv:1903.03894). arXiv. <https://doi.org/10.48550/arXiv.1903.03894>

## 6 Appendix

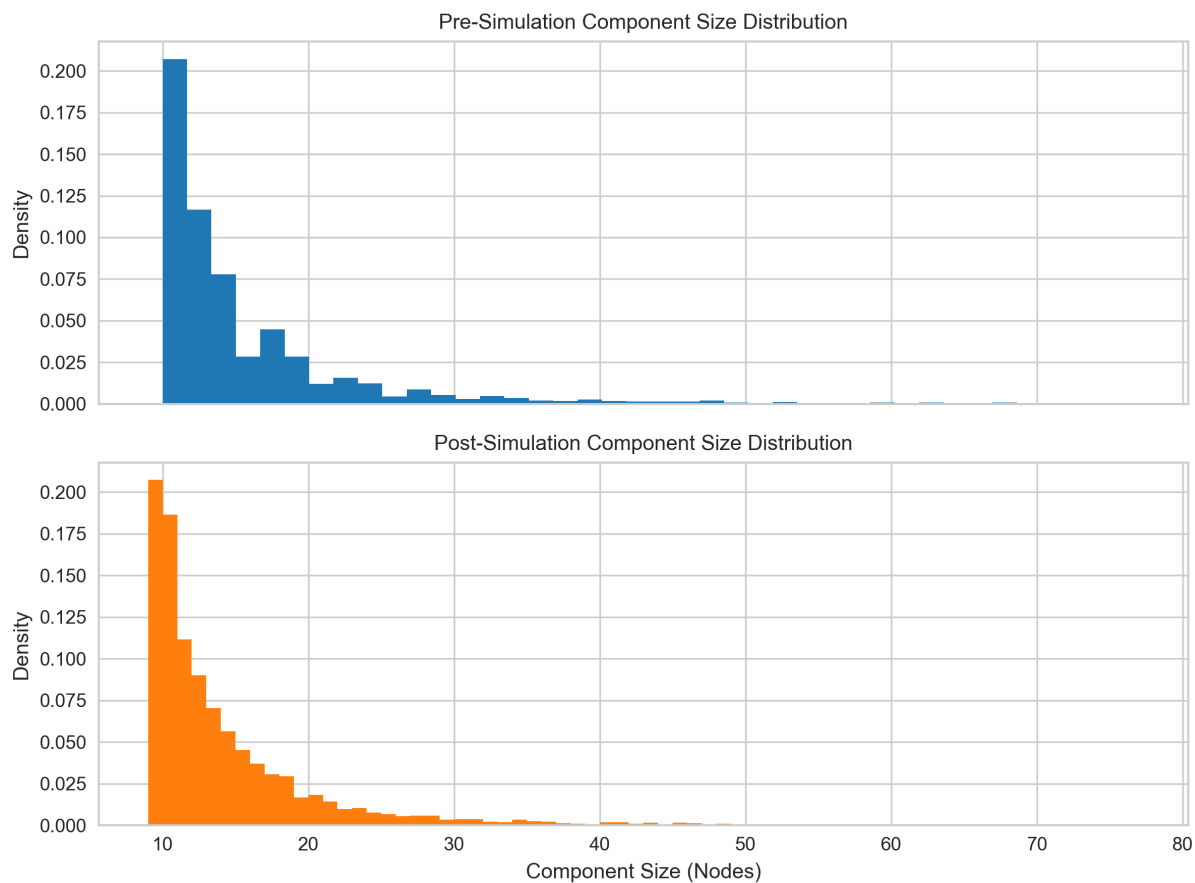


**Figure 8:** Distribution of component sizes before and after anomaly simulation.

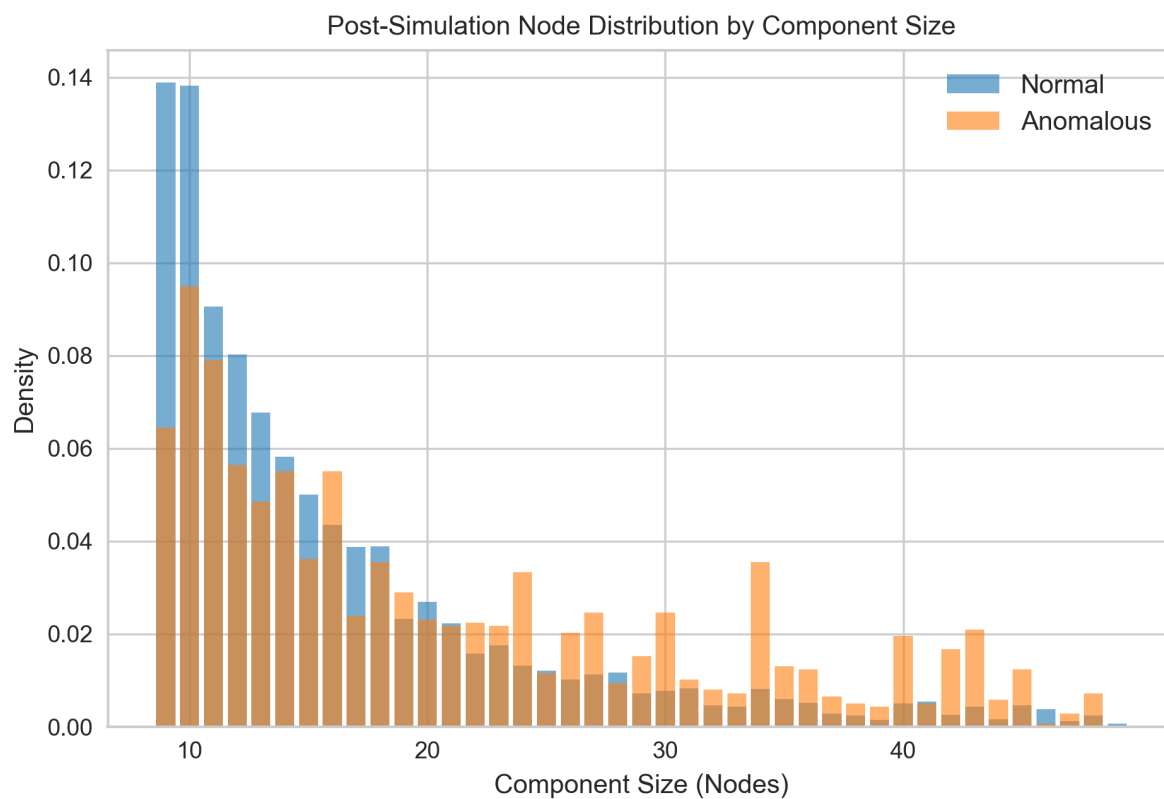


**Figure 9:** Distribution of anomalous nodes by component size before and after anomaly simulation.

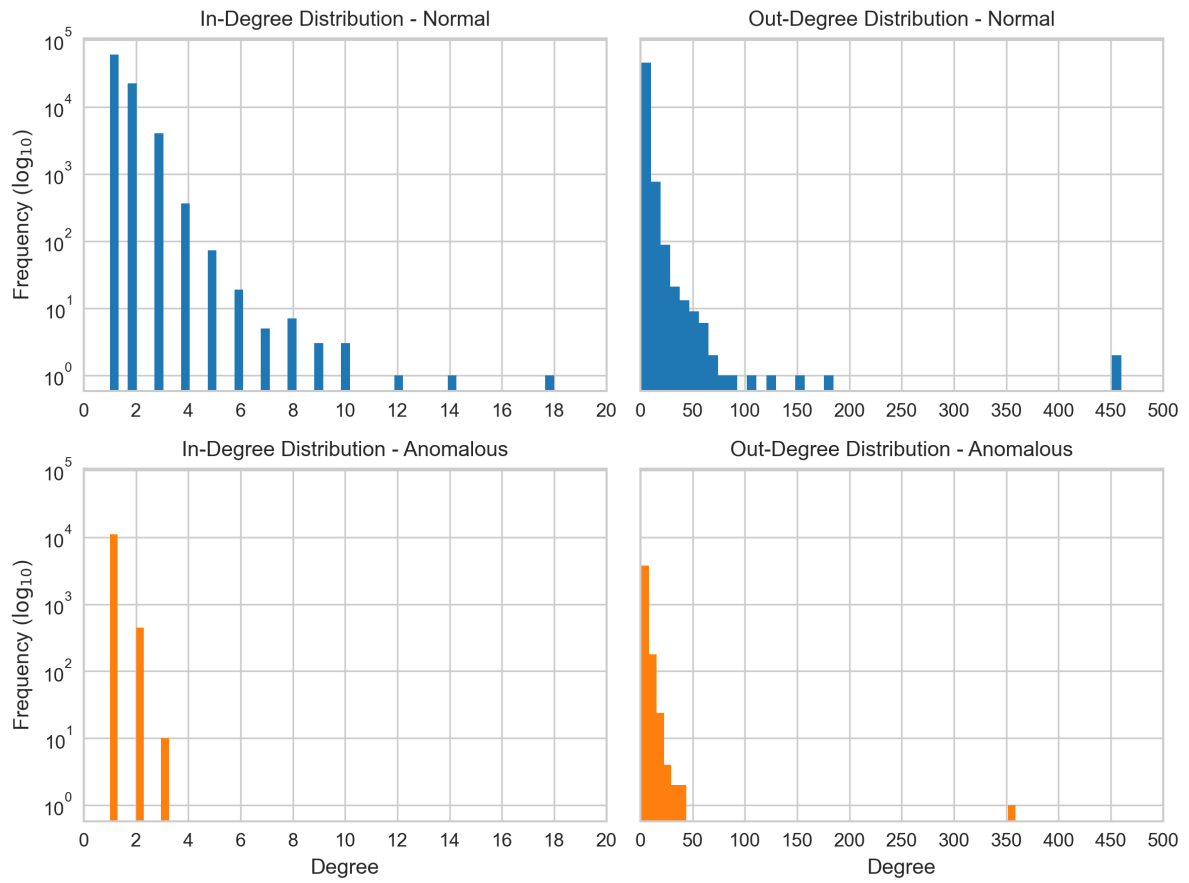


**Figure 10:** Distribution of node degrees before and after anomaly simulation.

**Table 2:** Neural architecture search space for GNN models - continuous.

Property	Min	Max
hidden layers	1	8
hidden channels	2	256
weight decay	0	0.01
dropout	0	0.5

**Table 3:** Neural architecture search space for GNN models - categorical.

Property	Choices
activation function	relu, gelu, leaky_relu
linear layer post-message passing	true, false
message passing aggregation	min, max, sum, mean
heterogeneous embedding aggregation	min, max, sum, mean